

ANALYSIS OF LOW-ALTITUDE LUNAR PROSPECTOR GAMMA RAY SPECTRA. T. H. Prettyman, J. J. Hagerty, R. C. Elphic, W. C. Feldman, T. E. Finnegan, D. J. Lawrence, G. W. McKinney, D. T. Vaniman, Los Alamos National Laboratory, Los Alamos, New Mexico (tprettyman@lanl.gov).

Introduction: Gamma ray spectra acquired by Lunar Prospector (LP) were analyzed to map the abundance of major oxides (MgO, Al₂O₃, SiO₂, CaO, TiO₂, and FeO) and radioactive elements (Th and K) for the entire lunar surface. Global maps of gamma ray spectra were constructed from data acquired at two altitudes (100 km and 30 km), while LP was in a circular, polar mapping orbit [1]. Spectral unmixing techniques similar to those used in optical spectroscopy were used to determine the composition of each map pixel. Neutron spectroscopy data, including the number density of neutrons slowing down within the surface and the effective atomic mass of the surface materials, were used to determine the coupling between neutron reactions and gamma ray production. A detailed description of the unmixing algorithm and its application to high-altitude (100 km) LP gamma ray data was recently published in *JGR* [2]. The unmixing algorithm simultaneously determines the abundance of all major- and radioactive elements, accounting for spectral interferences (such as spectral “contamination” of Fe by Al) not considered in previous studies.

Elemental scatter plots were used to compare the gamma ray remote sensing data to the lunar meteorite and sample data (soils and regolith breccias). The remote sensing and sample data were found to be generally consistent. Strong correlations in the sample data such as for K-Th and Al₂O₃-FeO were used to validate the unmixing algorithm. Remote sensing data that fell outside the range of the sample soils and regolith breccias revealed the presence of lithologies that were not well represented by lunar samples. For example, outliers in the FeO-Th and TiO₂-FeO scatter plots provided further evidence that the basalts in Western Procellarum are unique, and that significant changes in volcanism occurred over time [3]. The new elemental abundance data provide additional information needed to constrain lunar formation and evolution, including the ratio of volatile-to-refractory materials (K/Th ratio), constraints on the global heat balance (K and Th), characterization of mare basalts (Th, TiO₂ and FeO), probing the crust and mantle (composition of major impact basins such as South Pole-Aitken), and characterization of non-mare surface units. For example, our measurements of K/Th are consistent with findings by Taylor et al. [4] that the Moon is enriched in refractory elements to a greater degree than previously thought.

The spatial footprint of the spectrometer depends on altitude. At high altitude (100 km), the full-width-at-half-maximum (FWHM) of the response is approximately 2° of arc length along the spacecraft orbit;

whereas at low altitude (30 km), the FWHM is approximately 1°. Because the scale of the footprint is large compared to traverses at landing sites, lunar meteoritic data (specifically, the correspondence of the feldspathic lunar meteorites to the lunar highlands [5]) was used to calibrate models used in the analysis of high- and low-altitude data. Selected landing sites are sufficiently homogeneous that direct comparisons between remote sensing (especially, low altitude) and landing site sample data are appropriate for the purpose of ground truth [6,7]. Consequently, the low altitude data set has the dual benefit of improved spatial resolution and access to a more extensive range of calibration points that, in future work, can be exploited to improve the accuracy of the unmixing analysis, particularly for basalts. Since the precision of derived abundances depends on counting time, the combination of low- and high-altitude data is also useful for the analysis of elements with weak or poorly-resolved gamma rays (such as Ti). Future studies will focus on the analysis of gamma ray spectra for regions delineated by geological maps. Low- and high-altitude 0.5° maps of gamma ray spectra have been constructed for this purpose.

Low-altitude data analysis: The unmixing algorithm described in Prettyman et al. [2] was used, without modification, to analyze the low-altitude data. Elemental spectral components were generated for the 30-km average altitude, accounting for the reversal of the orientation of the spin axis relative to the high-altitude orbit. The procedures used to determine calibration constants and backgrounds were the same as in the high altitude case.

Results: Correlation plots (FeO-TiO₂) are shown, for example, in Fig. 1 for data binned on 5° pixels. The error bars indicate statistical precision (1σ). The distinct branch for high-Ti basalts is visible in the remote sensing data, especially in the low-altitude data set. Points with high FeO and low- to intermediate-Ti map to Western Procellarum. The uncertainty in FeO is such that the low- and high-altitude results are consistent within statistical variations and slightly higher than found in previous studies [6]. The lowest abundances of FeO and TiO₂ are found in the highlands and are consistent with the calibration assumptions.

Fig. 2 illustrates the difference in spatial resolution between the high- and low-altitude data sets. Features such as Compton-Belkovich and the detailed structure of the nearside Th “hot spot” appear prominently in the low-altitude data. Maps of FeO and TiO₂, shown in Fig. 3, were constructed by combining low- and high-altitude data. The procedure improves the statistical

quality of the map and preserves some of the high spatial resolution features found in the low-altitude data set. The spatial distribution of TiO_2 is consistent with Clementine spectral reflectance [8] and neutron spectroscopy data [9]; however, research continues on understanding differences in the magnitudes of TiO_2 abundances determined by different remote sensing techniques.

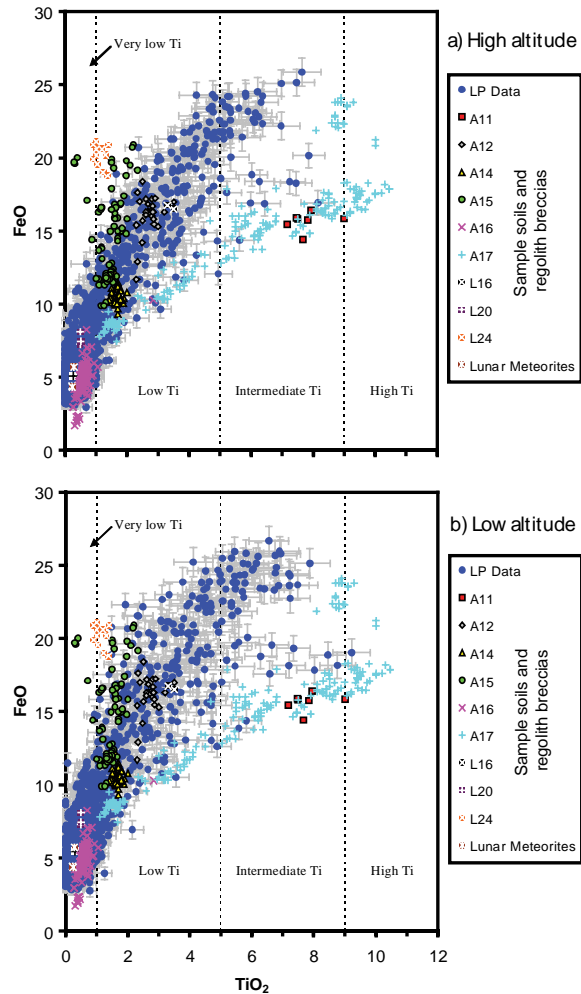


Fig. 1. Scatter plots of FeO versus TiO_2 determined from a) high altitude and b) low altitude gamma ray data binned on 5° equal area pixels. Sample and lunar meteoritic data are shown for comparison.

References: [1] Lawrence et al., *JGR*, 109, 2004. [2] Prettyman et al., *JGR*, 111, 2006. [3] Jolliff, *LPSC XXVI*, #2357, 2005. [4] Taylor et al., *GCA*, 70, 2006. [5] Korotev, *GCA*, 67(24), 2003. [6] Lawrence, *JGR*, 107(E12), 2002. [7] Gillis et al., *GCA*, 68(18), 2004. [8] Lucey et al., *JGR*, 105(E8), 2000. [9] Elphic et al., *JGR*, 107(E4), 2002.

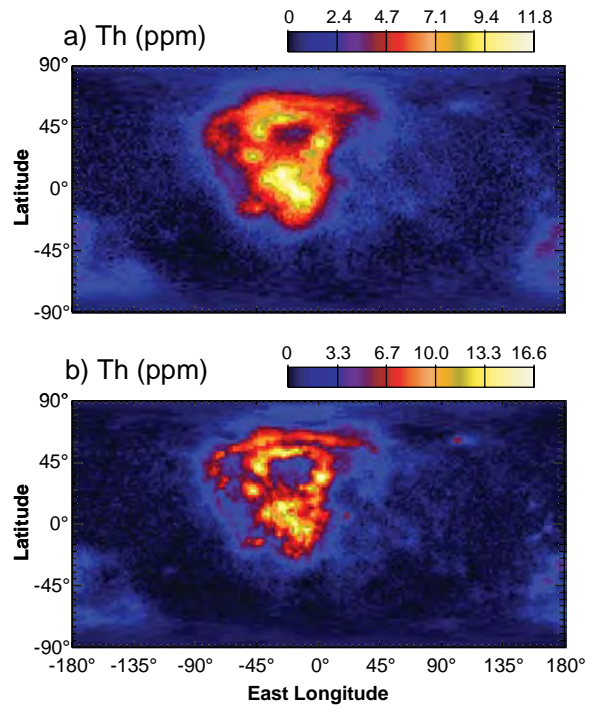


Fig. 2. Abundance of Th determined from data acquired at a) high altitude and b) low altitude. The spectra were binned on 2° equal area pixels.

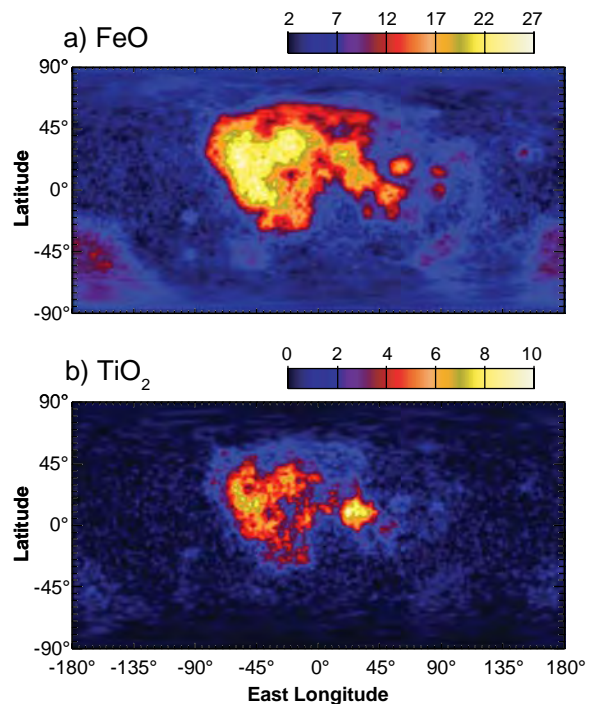


Fig. 3. 2° equal-area maps of a) FeO and b) TiO_2 determined by combining low- and high-altitude data.